Electronic Supplementary Information (ESI)

Biocompatible magnetic core-shell nanocomposites for engineered magnetic tissues

Laura Rodriguez-Arco,[*a] Ismael A Rodriguez,[b] Victor Carriel,[b] Ana B Bonhome-Espinosa,[a] Fernando Campos,[b] Pavel Kuzhir,[c] Juan D G Duran[a] and Modesto T Lopez-Lopez[*a]

[a] Department of Applied Physics, University of Granada, Faculty of Science, Campus de Fuentenueva, 18071 Granada, Spain, and Instituto de Investigación Biosanitaria ibs.GRANADA, Granada, Spain.

[b] Department of Histology (Tissue Engineering Group), University of Granada, Faculty of Medicine, Avenida de la Investigacion, 11, 18016 Granada, Spain, and Instituto de Investigación Biosanitaria ibs.GRANADA, Granada, Spain.

[c] Laboratory of Condensed Matter Physics, UMR No. 7336, University of Nice–Sophia Antipolis, CNRS, 28 Avenue Joseph Vallot, 06100 Nice, France

[*] Corresponding author email: l_rodriguezarco@ugr.es, modesto@ugr.es

- **Scanning electron microscopy (SEM)**

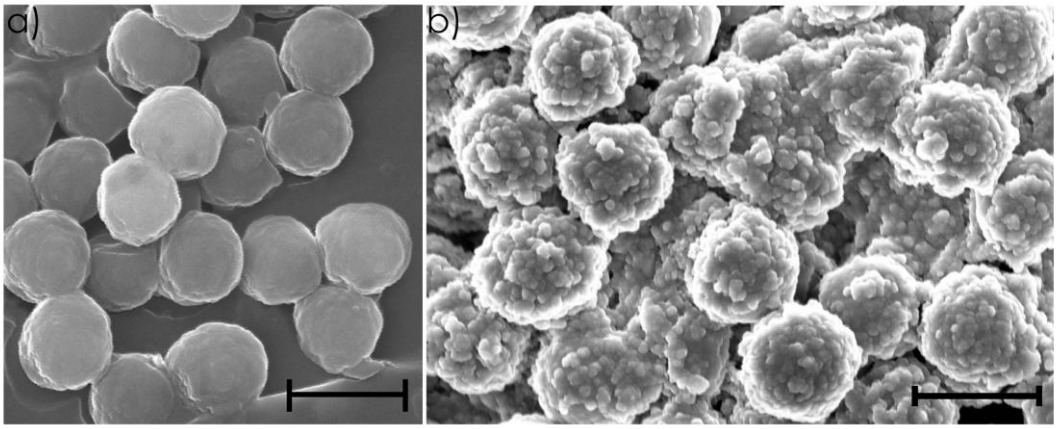

Fig. S1. Scanning electron microscopy photographs of the polymer core, Poly (a), and of Poly@Mag (b) composites (bar length = 1 µm).

The synthetic procedure resulted in the polymer cores fully and homogeneously coated with magnetic nanoparticles. More specifically, the smooth surface of the core (Fig. S1a) appeared completely covered with magnetic nanoparticles of diameter of 10-50 nm (Fig. S1b).

- **Fourier transform infrared spectroscopy (FTIR)**

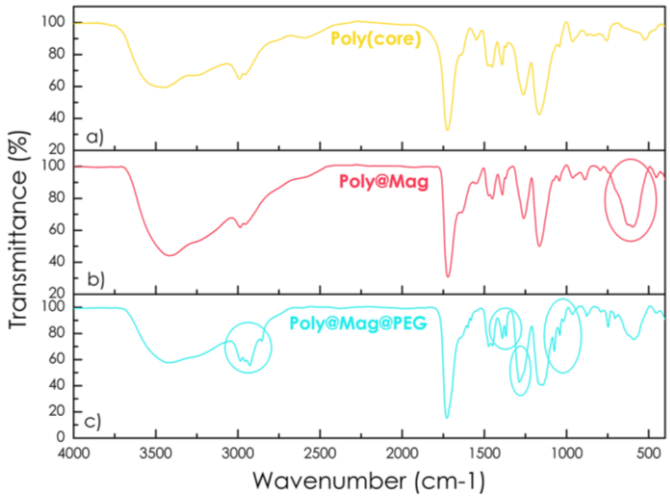

Fig. S2. FTIR spectra of (a) the nanocomposite core, Poly, and of (b) Poly@Mag and (c) Poly@Mag@PEG nanocomposites.

The material of the core, Poly, of our nanocomposites was a copolymer of methacrylic acid (MAA) and ethylene glycol dimethacrylate (EDMA). Its spectrum (Fig. S2a) showed the characteristic bands of alkyl (1260, 1370, 1480, and 2960 cm^{-1}), substituted alkenes (760, 960, and 1450 cm^{-1}), ester (1170 cm^{-1}), carboxyl acid and carboxylate (1720 and 1550 cm^{-1}) groups. The spectrum also showed the characteristic stretching broad band of the OH group (3200-3600 cm^{-1}) of the core functionalization. Coating of the acrylic polymer core with MNPs in Poly@Mag composites resulted in the appearance of the characteristic Fe-O vibration band at 590-630 cm^{-1}, which indicated the presence of iron oxide in the composites (Fig. S2b). Finally, for Poly@Mag@PEG composites, several new peaks appeared at 2925-2985 cm^{-1} corresponding to new alkyl groups. The characteristic band of $-CH_2-$ at 1290 cm^{-1} appeared to be more intense because of the coating with polyethylene glycol, PEG ($H-(O-CH_2-CH_2)_n-OH$). New weak but sharp signals appeared in the region 998-1220 cm^{-1} corresponding to the in-plane C-H and O-H deformations in PEG. Similarly, the combination band of O-C-H and C-O-H appeared at 1340-1440 cm^{-1} (Fig. S2c).

- **Thermogravimetric analysis (TGA)**

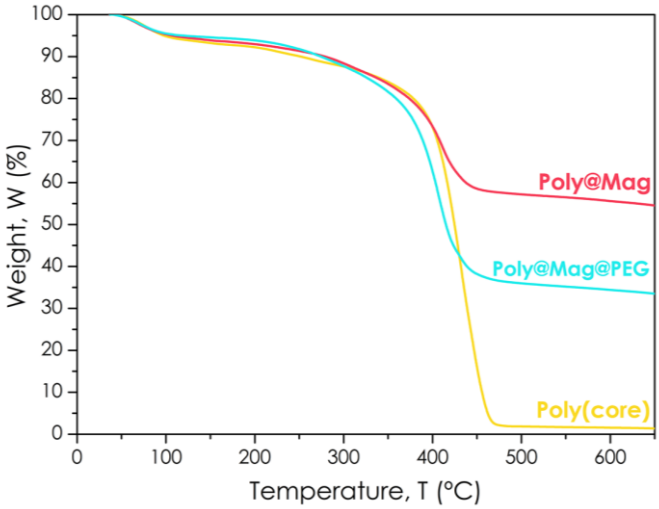

Fig. S3. TGA curves of the nanocomposite core, Poly (yellow), and of Poly@Mag (pink) and Poly@Mag@PEG (turquoise) nanocomposites.

All TGA curves (Fig. S3) exhibited an initial weight of loss of ~ 5% around 100 °C as a consequence of the evaporation of physically adsorbed water. The polymeric material of the core, Poly, completely degraded in the range 300-500 °C, as evidenced by the abrupt weight of loss in this range of temperatures until 0. Such a fall also appeared in the curve of Poly@Mag composites. However, in this second case an amount of ~50 wt% remained after heating. Such a residual weight after core degradation can be attributed to the inorganic shell of MNPs of the Poly@Mag composites. Finally in the case of Poly@Mag@PEG composites, the curve started to fall at lower temperature than for Poly@Mag sample, very likely because of the degradation of the outer PEG layer. The remained weight was ~30 wt% for Poly@Mag@PEG composites, because for this sample the relative amount of MNPs should have been lower due to the PEG coating.

- **X-Ray diffraction (XRD)**

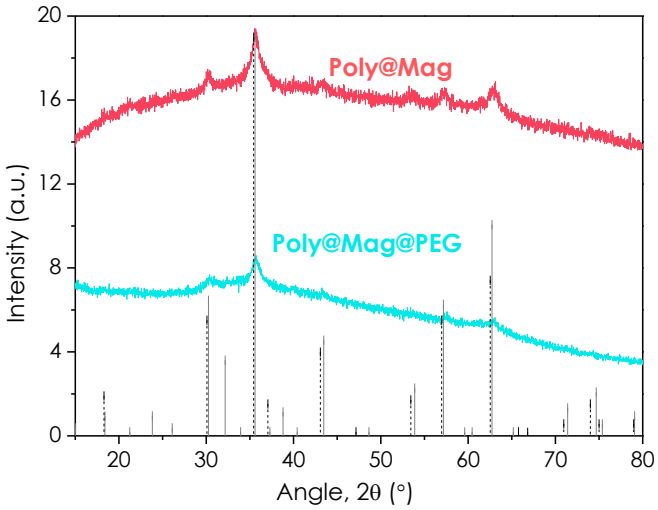

Fig. S4. XRD spectra of Poly@Mag (pink) and Poly@Mag@PEG (turquoise) nanocomposites with magnetite (dashed lines) and maghemite (solid lines) patterns.

In spite of the polymer core, Poly@Mag composites exhibited crystalline structure as shown by XRD analyses due to the maghemite grains of the magnetic shell (solid line pattern in Fig. S4). The XRD spectrum of Poly@Mag could also be fairly well fitted by magnetite pattern (dashed line in Fig. S4), because of its analogous inverse cubic spinel crystal structure. However, this is irrelevant from the magnetic point of view, because of the similar magnetic properties of magnetite and maghemite. PEG coating resulted in slight loss of crystallinity (see Fig. S4).

- **Transmission electron microscopy (TEM)**

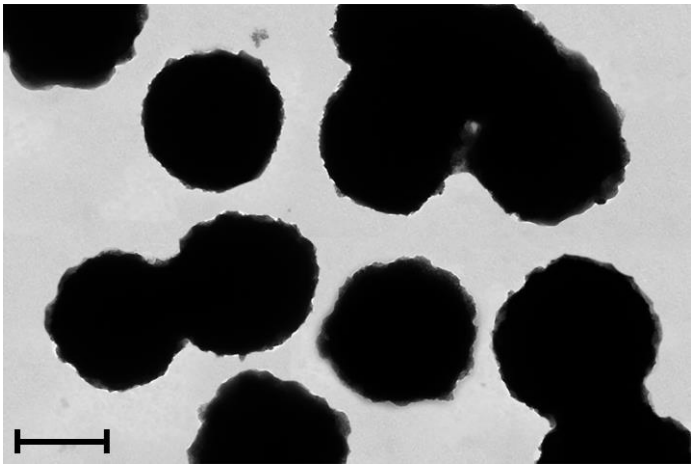

Fig. S5. Transmission electron microscopy (TEM) picture of a group of Poly@Mag@PEG nanocomposites (bar length = 500 nm).

Poly@Mag nanocomposites were coated by a layer of polyethylene glycol (PEG) to enhance their biocompatibility. The PEG shell in Poly@Mag@PEG appeared as a translucent thin film (thickness of a few nanometers) around the magnetic shell in TEM images (Fig. S5).

- **Ex vivo histological analyses of the magnetic engineered tissues**

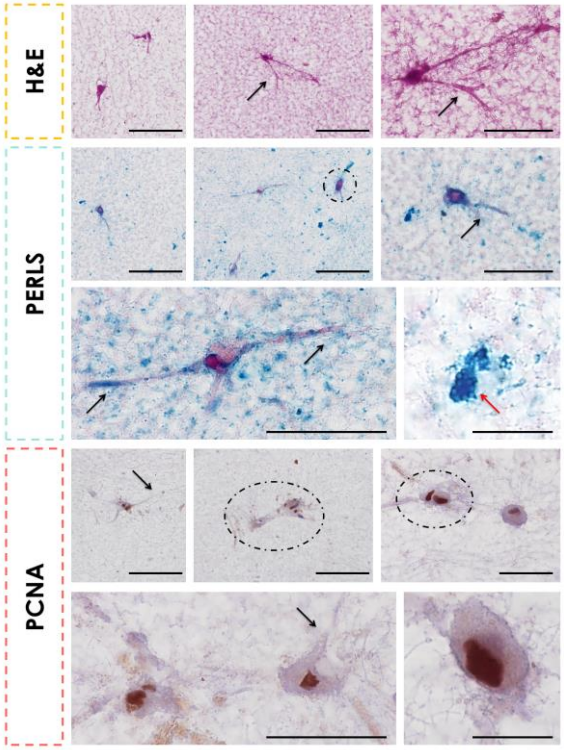

Fig. S6. Histological analyses of the magnetic engineered tissues.

We examined the morphology of the tissues by staining them with hematoxylin-eosin (H&E). Fibroblasts, which were found alone or forming cell clusters (circle), maintained their elongated shape and large *filopodia* (black arrows in Fig. S6). Perls' method (PERLS) allowed identification of the Poly@Mag@PEG nanocomposites due to their positive Prussian blue reaction. The nanocomposites appeared homogeneously distributed and were frequently observed near the cell surface, around the perinuclear cytoplasm and the large *filopodia* of the fibroblasts (Fig. S6). High magnification image of PERLS revealed the characteristic spherical and regular nanostructure of the composites (red arrow in Fig. S6). Tests for the proliferating cell nuclear antigen (PCNA) showed positive immunohistochemical reaction of PCNA in the nuclei of individual or grouped fibroblast (circle in Fig. S6), which was an indicator of cell proliferation.

- **Magnetic response of the engineered magnetic tissues**

The prepared magnetic tissues were magnetic field-responsive and moved towards the regions of higher magnetic field when placed near a permanent (neodymium) magnet (magnetic field gradient of 10 $mT \cdot mm^{-1}$) as seen in Video 1.

- **Magnetization curve of substitute tissue**

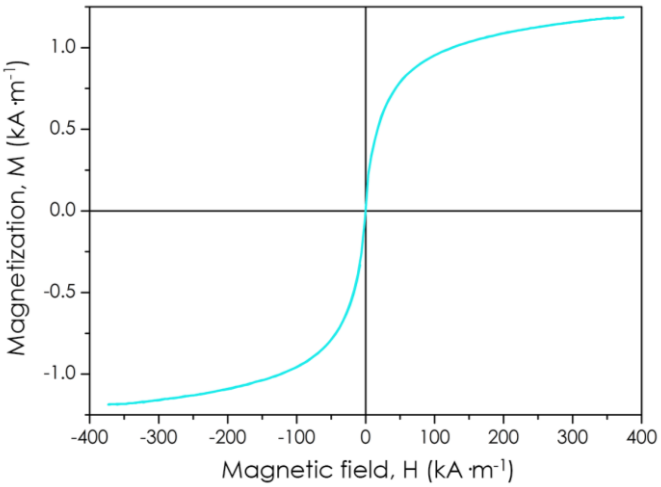

Fig. S7. Magnetization curve of the engineered tissue prepared with Poly@Mag@PEG nanocomposites.

The artificial magnetic tissues prepared with Poly@Mag@PEG composites showed soft ferromagnetic behavior (Fig. S7), with a much lower saturation magnetization than the nanocomposites (~ 1.5 kA·m^{-1}). Using the magnetic mixing law we estimated the volume fraction of magnetic material in the tissues to be ~ 0.3 vol %.

- **Mechanical properties**
  - **Amplitude sweep for loss modulus**

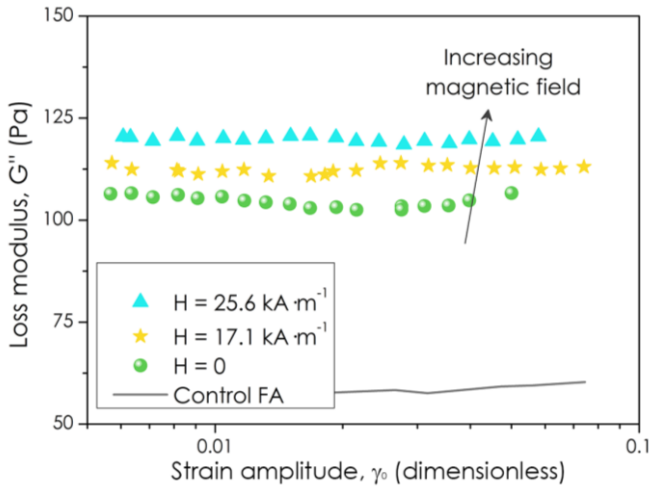

Fig. S8. Loss modulus, G'', as a function of the amplitude of the applied oscillatory strain.

The loss modulus (G'') of the artificial magnetic tissues remained almost constant for all the range of oscillatory strains (Fig. S8). G'', connected to the dissipation of energy upon oscillatory stress, was always lower than the storage modulus (G'), suggesting a solid-like behavior for all the tissues. G'' was much higher for the tissues containing Poly@Mag@PEG composites than for the control fibrin-agarose tissue (FA) with no composites, as it happened for G'. This can be explained by an increase of the internal friction due to the linkage between the composites and fibrin fibers. However, the most interesting result was that G'' increased ~15% when the magnetic field was applied.

- **Frequency sweep**

The increase of G' and G'' with the magnetic field was maintained over the whole range of frequencies (*f*) of the oscillatory stimulus (Fig. S9). G' showed a smooth increased reaching a *plateau* for $f > 1$ Hz. In contrast, for $f < 1$ Hz, G'' remained almost constant, followed by an abrupt increase for $f > 1$ Hz. This indicated stronger dissipation of energy at higher frequencies. The values of G' were higher than those of G'' over the entire range of studied frequencies. Both moduli were much larger than those of the FA control tissue.

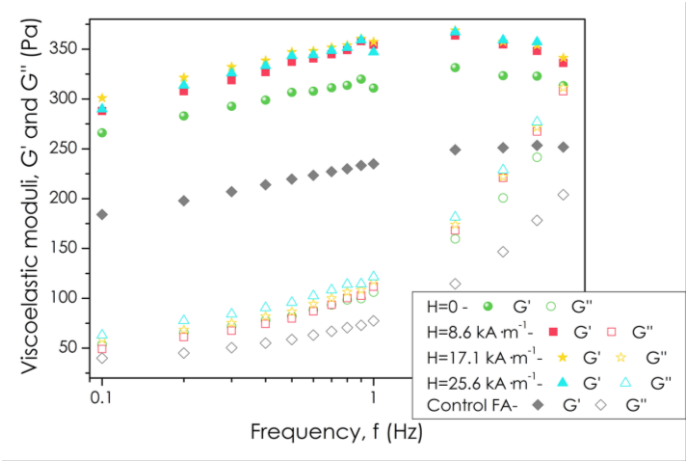

Fig. S9. Storage, G', and loss, G'', moduli as a function of the frequency of the applied oscillatory strain.

- **Time-dependent *in vivo* biocompatibility of Poly@Mag@PEG composites and magnetic substitutes**

  - **Magnetic response of samples from organs**

Table S1. Magnetic response of samples from different parts of the body of mice after 1, 2 and 3 weeks. "NM" and "M" stand for "non-magnetic" and "magnetic" respectively. Results for three experimental groups: (a) control group of healthy mice, (b) mice subcutaneously injected with a suspension of Poly@Mag@PEG composites, and (c) mice with implants of Poly@Mag@PEG magnetic tissues.

	Organ →	Interscapulum	Liver	Spleen	Lungs	Kidneys
Experimental group ↓	Time ↓					
(a) Control group	Week 1	NM	NM	NM	NM	NM
	Week 2	NM	NM	NM	NM	NM
	Week 3	NM	NM	NM	NM	NM
(b) Suspension of Poly@Mag@PEG nanocomposites	Week 1	**M**	NM	NM	NM	NM
	Week 2	**M**	NM	NM	NM	NM
	Week 3	**M**	NM	NM	NM	NM
(c) Engineered magnetic tissues of Poly@Mag@PEG nanocomposites	Week 1	**M**	NM	NM	NM	NM
	Week 2	**M**	NM	NM	NM	NM
	Week 3	**M**	NM	NM	NM	NM

Only the samples taken from the interscapular region of mice exhibited a magnetic response after 1, 2 and 3 weeks. Therefore, we can conclude that Poly@Mag@PEG composites remained in the interscapular region and did not migrate to other organs on the timescale of the *in vivo* experiments. This happened both when the nanocomposites were injected subcutaneously, and when the magnetic engineered tissues containing them were implanted.